MOLECULAR AND CELLULAR BIOLOGY, Sept. 2009, p. 4679–4690 Vol. 29, No. 17
0270-7306/09/$08.00+0 doi:10.1128/MCB.00297-09

The *Drosophila* Metastasis Suppressor Gene *Nm23* Homolog, *awd*, Regulates Epithelial Integrity during Oogenesis▽‡

Julie A. Woolworth,† Gouthami Nallamothu,† and Tien Hsu*

Department of Pathology and Laboratory Medicine and Hollings Cancer Center, Medical University of South Carolina, Charleston, South Carolina 29425

Received 6 March 2009/Returned for modification 7 April 2009/Accepted 24 June 2009

The expression levels of the metastasis suppressor gene *Nm23* have been shown to correlate positively or inversely with prognosis in different cancer cohorts. This indicates that *Nm23* may be needed at different expression levels and may function differently in various tissues. Here we report a novel epithelial function of the *Drosophila melanogaster* homolog of human *Nm23*, *abnormal wing discs* (*awd*). We show a dynamic expression pattern of the Awd protein during morphogenesis of the *Drosophila* follicle cells during oogenesis. Loss-of-function *awd* mutant cells result in the accumulation and spreading of adherens junction components, such as *Drosophila* E-cadherin, β-catenin/Armadillo, and α-spectrin, and the disruption of epithelial integrity, including breaking up of the epithelial sheet and piling up of follicle cells. In contrast, overexpression of *awd* diminishes adherens junction components and induces a mesenchymal-cell-like cell shape change. The gain-of-function phenotype is consistent with a potential oncogenic function of this metastasis suppressor gene. Interestingly, we demonstrate that the epithelial function of *awd* is mediated by Rab5 and show that the Rab5 expression level is downregulated in *awd* mutant cells. Therefore, *awd* modulates the level and localization of adherens junction components via endocytosis. This is the first demonstration of an in vivo function of *Nm23* family genes in regulating epithelial morphogenesis.

Nm23 was first identified as a transcript that was downregulated in highly metastatic derivatives of a murine melanoma cell line, K-1735 (43). Later studies revealed that *Nm23* consists of a family of eight related genes in mammals (24). The 1 and 2 isoforms (human H1 and H2) are the most closely related and are the ones most often implicated in tumor progression. They are also evolutionarily highly conserved. The *Drosophila melanogaster Nm23* gene, *abnormal wing discs* (*awd*), shares 78% amino acid identity with either human H1 or H2 (5). The *awd* lethal phenotype can be rescued by exogenously expressed Nm23-H2 (51). Early studies of *awd* also led to the finding that *Nm23* genes encode nucleoside diphosphate kinase activity, which converts nucleoside diphosphates to nucleoside triphosphates using ATP as the phosphate source (5, 50).

In xenograft and allograft models, *Nm23* has been shown to inhibit metastasis, but not primary tumor growth, of cells from human breast cancer, murine melanoma, rat colon cancer, and human oral squamous cancer (reviewed in reference 38). However, in clinical cancer samples, the function of *Nm23* is somewhat murkier. While in earlier breast cancer studies there were statistically significant correlations between reduced *Nm23* expression levels and some criteria of metastasis (reviewed in reference 20), in later studies no clear correlations could be discerned (1, 2, 16, 39, 42). Furthermore, in other cancer cohorts, particularly those of ovarian cancers, upregulated *Nm23* levels have been correlated with poor prognosis (19, 29), suggesting an oncogenic function for *Nm23*. While many of the discrepancies can be attributed to the method used (Northern analysis versus immunohistochemistry, for example) or the quality of the reagents (antibody specificity, for example), these observations also suggest that the physiological and developmental functions of the *Nm23* family of genes operate in a defined range of expression levels. Thus, either overexpression or reduced expression of *Nm23* can result in abnormal cellular phenotypes. Homozygous *Nm23-M1* knockout mice exhibited delayed mammary gland development but were otherwise healthy (3). These mice also conferred an elevated metastasis potential when induced for hepatocellular-carcinoma formation (7). However, these results did not shed light on the physiological functions of the Nm23 family of proteins. More recently, the *Xenopus laevis* Nm23-X4 isoform has been shown to negatively regulate retinal gliogenesis by inhibiting p27Xic1, a *Xenopus* cyclin-dependent kinase inhibitor (33). Continuing studies of this system should determine whether this function is conserved in other family members and in other tissue systems.

To date, the most physiologically relevant function of *Nm23* was revealed by genetic studies of *Drosophila* (reviewed in reference 35). *awd* was identified in a genetic screen for genes involved in imaginal-disc development (9, 10). It was also shown that primordial ovaries from *awd* mutants failed to develop when transplanted into wild-type larvae, although mutant germ cells from early embryos were capable of producing normal eggs in wild-type surrogates (9). Since in the latter case, the wild-type surrogate embryos provided the somatic cells to form the functional ovaries, the observation suggested that *awd* may play a specific role in the development of somatic follicle cells in the egg chamber (35). This interesting finding

* Corresponding author. Mailing address: Medical University of South Carolina, Hollings Cancer Center, 86 Jonathan Lucas St., Room 330, Charleston, SC 29425. Phone: (843) 792-0638. Fax: (843) 792-5002. E-mail: hsut@musc.edu.

† These authors contributed equally to this work.

‡ Supplemental material for this article may be found at http://mcb.asm.org/.

▽ Published ahead of print on 6 July 2009.

may now be explained by our current study. More recently, in a genetic screen for second-site mutations that exacerbate the neurological phenotype of a temperature-sensitive *dynamin* mutant (paralysis at 29°C due to defects in endocytosis-mediated neurotransmitter uptake), Krishnan et al. (23) isolated three lines of such *dynamin* enhancers. All three are alleles of *awd*. This suggests that the functional relationship between *awd* and endocytosis is exceedingly specific and almost exclusive. Our own subsequent studies (8, 36) demonstrated that the endocytic activity of Awd is not restricted to the neuronal function; that is, Awd can downregulate epithelial-cell motility by promoting internalization of chemotactic signaling receptors. In the tracheal tubules, *awd* mutants exhibit surface overaccumulation of the fibroblast growth factor (FGF) receptor (encoded by the *breathless* gene) and ectopic tubule cell migration (8). In the ovary, Awd is normally downregulated in a group of epithelial cells (the border cell complex) that delaminates from the epithelium and migrates through the germ cell complex to reach the developing oocyte. Forced expression of Awd in border cells reduced the level of the chemotactic platelet-derived growth factor/vascular endothelial growth factor (PDGF/VEGF) receptor (Pvr) and inhibited cell movement (36). These functions provide a plausible role of *Nm23* in downregulating metastasis.

In the course of studying the function of Awd during oogenesis, we also noted a dynamic subcellular-localization pattern of the Awd protein in the somatic follicle cells that surround the germ cells in the ovary, indicating a role in epithelial morphogenesis. In this report, we show that *awd* regulates the distribution of adherens junction components and, therefore, the epithelial integrity. These findings also provide the explanation for the original observation suggesting a somatic-cell-specific oogenic function for *awd* more than 20 years ago (9, 35).

MATERIALS AND METHODS

***Drosophila* strains.** *y w*; *UAS-awd* and *y w*; *hsp-awd* strains, carrying the *awd* open reading frame under the control of a *UAS* (upstream activation sequence) enhancer and a heat shock promoter, respectively, have been described previously (8, 36). To generate *awd* RNA interference constructs, tail-to-tail tandem copies of 5′ portions of the *awd* open reading frame were cloned in the *pCaSpe-hs* or the *pUAS* vector under the heat shock promoter or the *GAL4/UAS* binary control, respectively. These expression vectors were used to transform the *y w* flies. Transgenic flies carrying wild-type, constitutively active (CA), and dominant negative (DN) variants of the *UAS-YFP-Rab5* and *UAS-YFP-Rab11* fusion genes (where YFP is yellow fluorescent protein) were obtained from the Bloomington Stock Center and have been described previously (53). Briefly, cDNAs for wild-type *Rab5* and *Rab11* were generated using reverse transcription-PCR from total embryonic RNA preparations. CA and DN variants were generated by in vitro mutagenesis. The coding sequences were fused to the 3′ end of the *YFP* open reading frame and cloned into the *pUAS* transgenic vector. Localizations of the wild-type and CA proteins to the proper endocytic compartments in the photoreceptors and in cultured cells were verified. On the other hand, DN mutant proteins were shown to be mislocalized, consistent with their mutant nature. Hemagglutinin-Arf6 fusion genes were generous gifts of C. D'Souza-Schorey of the University of Notre Dame (40). The $GAL4^{55B}$ transgenic line expresses GAL4 in the anterior population of the main-body follicle cells starting at stage 8 (30, 31). The protein-null *awd* allele awd^{j2A4} is a P-element insertion, as described previously (8, 23). awd^{KRS6} is a deletion allele that removes a 788-bp region encompassing the entire protein-coding domain (46). The mutant awd^{j2A4} allele, located at the tip of the chromosome arm 3R, was crossed onto chromosome 3R carrying the *Saccharomyces cerevisiae* recombination site FRT^{82B} at the base of the chromosome arm. The mitotic mutant clone was induced by crossing the awd^{j2A4}, FRT^{82B} fly with a transgenic strain carrying the wild-type FRT^{82B} chromosome and the *UAS-FLP* recombinase transgene under the control of the *e22c-GAL4* driver. *e22c-GAL4* directs expression specifically in follicle cells and not in germ line cells. FLP recombinase induces recombination at the *FRT* sites between *awd* and wild-type chromatids during mitosis, resulting in homozygous *awd* mutant and sister wild-type cells. $awd^{K\text{-}pn}$ is a neomorphic nonlethal allele that encodes a P97S mutation. The complete genotypes of the *awd* mutant stocks are *y w*; $P\{w+\}awd^{j2A4}/TM3$, Sb^1, *y w*; awd^{KRS6} $e^s/TM3$, Sb^1 Ser^1, y^+ and ca^1 $awd^{K\text{-}pn}$. They were obtained from the Bloomington Stock Center. The $hsp\text{-}awd^{wt}$ transgene (where wt is the wild type) was used to rescue the lethality of awd^{KRS6} when grown at 29°C. The homozygous *hsp-awd*; awd^{KRS6} female adult survivors were then examined for egg chamber phenotypes after incubation at the restrictive temperature of 18°C. The $hsp\text{-}awd^{H119A}$ mutant transgene was generated by in vitro mutagenesis and used to transform *y w* flies.

Transgene and RNA duplex induction. For the *GAL4/UAS* expression system, the flies were conditioned in the presence of live baker's yeast at 25°C for 2 days and then incubated at 29°C for 3 days before dissection. For heat shock-induced expression, flies were conditioned in the presence of live baker's yeast at 25°C for 2 days and then heat treated twice daily at 37°C for 30 min for a total of 3 days. Ovary dissection was carried out ~2 h after the final heat treatment.

Immunohistochemistry. Ovaries were dissected into 1× Ringers solution (182 mM KCl–46 mM NaCl–3 mM $CaCl_2$–10 mM Tris-HCl, pH 7.2) containing 1% bovine serum albumin and fixed in 4% paraformaldehyde in phosphate-buffered saline (PBS) overlaid with heptane. Subsequent washes and incubations were performed with PBS–NP-40 (1× PBS containing 0.5% NP-40). Primary-antibody incubation was performed at 4°C overnight. Protein A-purified polyclonal rabbit anti-Awd (3 mg/ml) was used at a 1:1,000 dilution and has been described previously (8). Mouse monoclonal anti-Arm (N27A1), rat monoclonal anti-*Drosophila* E-cadherin (DE-cadherin) (DCAD2), mouse monoclonal anti-α-spectrin (3A9), mouse monoclonal anti-Crumbs (Crb) (Cq4), mouse monoclonal anti-integrin PSβ (CF.6G11), and mouse monoclonal anti-Discs large (Dlg) (4F3) were obtained from the Developmental Studies Hybridoma Bank. Rabbit polyclonal anti-Lethal(2) giant larvae (Lgl) and rabbit anti-dystroglycan (Dg) antibodies are generous gifts of D. Grifoni of the University of Bologna (18) and W. M. Deng of Florida State University (11), respectively. Other commercially available primary antibodies used were mouse monoclonal anti-Rab5 (610281; BD Biosciences) and mouse monoclonal anti-β-galactosidase (G4644; Sigma). Alexa Fluor 546-phalloidin and To-Pro-3 are from Invitrogen/Molecular Probes (A22283 and T3605, respectively). Alexa Fluor 488-, 546-, and 647-conjugated secondary antibodies (Invitrogen/Molecular Probes) were used at a 1:200 dilution, and incubation was performed for 2 h at room temperature. For Lgl and Dg double staining with Awd (all using rabbit polyclonal antibodies), the anti-Awd antibody was preconjugated with Alexa Fluor dye using a Zenon rabbit immunoglobulin G labeling kit (Invitrogen/Molecular Probes) and used directly without secondary antibody. Samples were analyzed using an Olympus IX70 microscope equipped with Fluoview 300 confocal capability. Digital images were processed using Photoshop software without biased manipulations.

RESULTS

Awd expression in epithelial cells is dynamic. *Drosophila* follicle cells provide an excellent model for studying epithelial establishment and maintenance. Each *Drosophila* egg chamber contains a germ cell complex—one oocyte and 15 nurse cells—that originates from a germ line stem cell (12). A single layer of epithelial follicle cells envelops the germ cell complex (Fig. 1A). The follicular epithelium mechanically supports the integrity of the egg chamber and communicates with the germ cells to provide positional cues for the developing oocyte. These functions rely on a dramatic morphogenic event at stage 9, in which ~95% of the 1,000 or so follicle cells move posteriorly as a sheet until they precisely envelop the oocyte. These are called columnar or main-body follicle cells. The remaining ~5% of the anterior follicle cells become stretched and squamous. The follicular epithelium exhibits the typical epithelial polarity exemplified by markers such as the adherens junction component DE-cadherin, located at the apicolateral membrane domain, and Lgl, located at the basolateral domain (Fig. 1B).

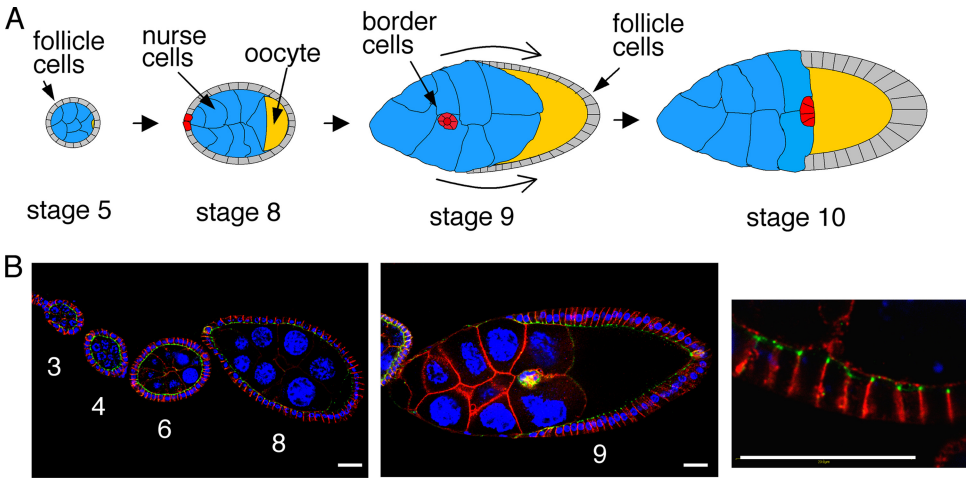

FIG. 1. Egg chamber developmental stages and epithelial structure. (A) Illustration of representative stages of *Drosophila* egg chambers. Major cell types are marked. The curved arrows at stage 9 indicate the posterior movement of the epithelial sheet until the columnar follicle cell sheet exactly covers the oocyte at stage 10. (B) The left and middle panels show stage 3 to 8 and stage 9 egg chambers, respectively, stained for DE-cadherin (green), Lgl (red), and nuclei (To-Pro, blue). A close-up view (right panel) of stage 8 follicle cells shows the typical polarized distribution of DE-cadherin in a "two-dot" pattern, marking the apicolateral junctions of each cell, and Lgl in the basolateral membrane domains. Bar, 20 μm.

We observed that Awd is expressed in the follicular epithelium in a dynamic pattern. In early egg chambers (pre-stage 5), Awd is expressed throughout the follicle cell body (Fig. 2A). After stage 5, Awd gradually accumulates to the basal side of the cell (Fig. 2A). Basal localization becomes prominent at stage 6 and is firmly established after stage 8. At stage 10, Awd is associated exclusively with the basal domain of the cells (Fig. 2B). The basal localization of Awd can be seen clearly as Awd overlaps with β-integrin in these cells (Fig. 2C). Stage 6 is a critical time in epithelial morphogenesis, as these follicle cells cease to proliferate and begin to adopt a columnar shape. The dynamic expression pattern of Awd in the epithelial follicle cells (Fig. 2D) raised the possibility that Awd may regulate epithelial morphogenesis. We set out to test this hypothesis.

***awd* mutant cells show accumulation of adherens junction components.** Homozygous *Drosophila awd* mutants are lethal. In order to study the loss-of-function phenotype in the adult follicular epithelium, we generated homozygous mutant follicle cell clones in the heterozygous animals by using the FLP/FRT system. The mutant allele *j2A4* is a P-element insertion that results in a loss of protein expression (8, 23). Figure 3A shows a wild-type stage 9 egg chamber stained for *Drosophila* β-catenin (Armadillo, or Arm) and Awd. Awd is localized to the basal side, while Arm shows a typical accumulation at the apicolateral loci of the awd^+ cells. In an *awd* mutant clone (identified as cells lacking Awd staining) (compare Fig. 3A, B, and C), Arm spreads to the apical membrane domain, and the overall lateral membrane level also increases. A similar accumulation is observed for DE-cadherin (Fig. 3D). Closer examination of the mutant clones revealed an abundance of Arm-containing vesicles in the *awd* mutant cells compared to the level in the normal cells, which show typical Arm localization to the apicolateral surface, with enrichment in the three-cell junctions and little cytoplasmic aggregation (Fig. 3C′, insets). The adherens junction-linked cytoskeletal component α-spectrin is also overaccumulated on the lateral domain (Fig. 3E). We then examined the organization of the DE-cadherin–Arm complex in the *awd* mutant cells. Wild-type or *awd* mutant clones were doubly stained for DE-cadherin and Arm (Fig. 3F). In wild-type cells, there is an expected colocalization of DE-cadherin and Arm in the apicolateral membrane domain. There are also scattered DE-cadherin and Arm in separate basolateral cortical loci (Fig. 3F). A recent report has indicated that β-catenin uncomplexed with E-cadherin can remain at the cell periphery by tethering to the microtubule minus ends (32). In *awd* mutant cells, DE-cadherin and Arm overaccumulate together in the apical domain. However, in the basolateral domain and in the cytoplasm, vesicles containing DE-cadherin or Arm alone and vesicles containing both components are observed (Fig. 3F). This indicates that DE-cadherin and Arm spread to the apical domain as a complex. Separate DE-cadherin and Arm in the cytoplasm may result from an internalization of isolated proteins from the cell cortex, from sorting after the complex is internalized, or both. It is not yet clear how the non-membrane-bound β-catenin becomes associated with transport vesicles, although evidence has suggested that caveolin may recruit β-catenin to the lipid rafts prior to internalization (17).

Western blot analysis of the ovary extracts isolated from wild-type, *hsp-awd* overexpression, and $hsp\text{-}awd^{sb}$ (knockdown) flies did not show grossly altered protein levels for DE-cadherin, Arm, or α-spectrin (see Fig. S1 in the supplemental material). This indicates that Awd regulates mainly the cytoplasm-membrane translocalization of these proteins and not their expression levels. Elevated staining of these proteins in *awd* mutant cells probably occurs because indirect immunofluorescence favors aggregated antigens, such as those concentrated at the membrane domains or in vesicles. Wild-type cells may contain an abundant cytoplasmic pool of the adherens junction components undetected by our immunofluorescence settings.

We also determined that the expression of the apical marker

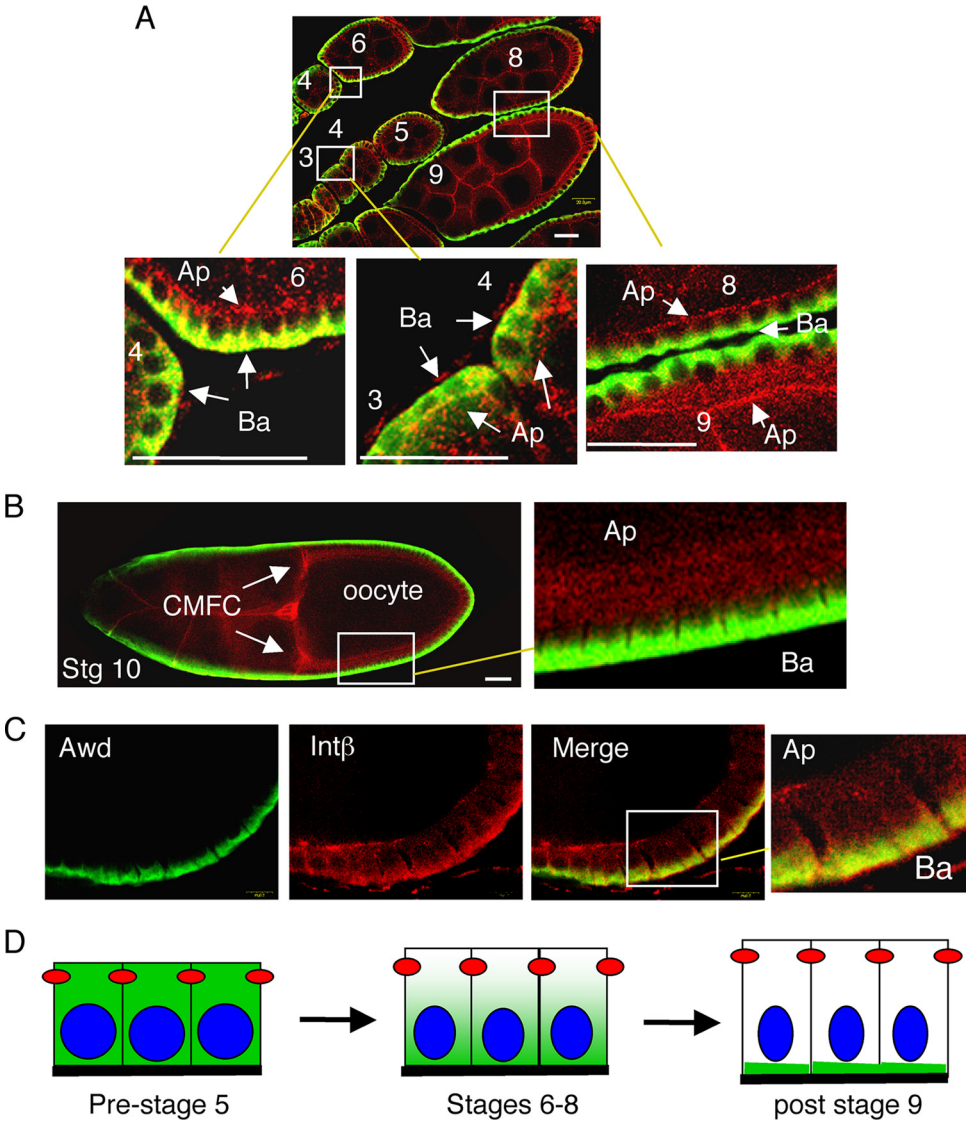

FIG. 2. Dynamic expression of Awd in follicle cells. (A and B) Ovaries were stained for Awd (green) and Rac (red), the latter to mark the outline of follicle cells. (A) An expanded view is shown in the top panel, with three zoomed-in views of different stages shown in the bottom panels. The numbers indicate the stages of the egg chambers. Ap and Ba indicate the apical and basal sides of the cells, respectively. Awd gradually moves away from the apical domain after stage 5. Bars, 20 μm. (B) Stage (Stg) 10 egg chamber. CMFC, centripitally migrating follicle cells. Bar, 20 μm. (C) Basal localization of Awd (green) is demonstrated by double staining with β-integrin (Intβ) (red). A portion of the stage 10 follicular epithelium is shown. (D) Diagram depicting the subcellular relocalization of Awd (green). Adherens junctions are shown in red.

Crumbs (Crb) is moderately increased but not overtly altered (Fig. 3G). The basal marker Dg revealed that the basal adhesion of *awd* mutant cells is defective (seen as wavy basal membranes [Fig. 3H]) but that the basal localization of Dg itself is not altered. The basolateral markers Dlg and Lgl are not altered (Fig. 3I and J). Therefore, Awd appears to be a specific regulator of localization of adherens junction components.

***awd* mutant follicle cell clones show disruption of epithelial characteristics.** The mutant cells shown in Fig. 3B become flattened but remain adhered to their neighbors. In clones containing a large number of mutant cells, a more prominent disruption of epithelial integrity is observed (Fig. 3E and K to N). Figure 3E shows a piling-up phenotype. Figure 3K′ shows a stretched epithelium, and in more severe cases (Fig. 3K″ and L), the epithelial continuity is broken. This indicates a weakening of the adherens junctions. The defect is likely exacerbated during the epithelial-sheet movement after stage 8, in which the posteriorly moving epithelial sheet stretches the anterior follicle cells into a squamous shape. Weakened adherens junctions in cells overaccumulating DE-cadherin and Arm indicate that these overaccumulated adherens junction components are not engaged in effective cell adhesion and may disrupt the normal cell-cell adhesion.

In addition to epithelial breakup, adenoma-like epithelial piling is frequently observed (Fig. 3L and M). In the most severe phenotype, the follicle cell sheet invades the germ cell proper (Fig. 3N). The occurrences of these phenotypes are summarized in Fig. 4. The severity of the phenotypes correlates

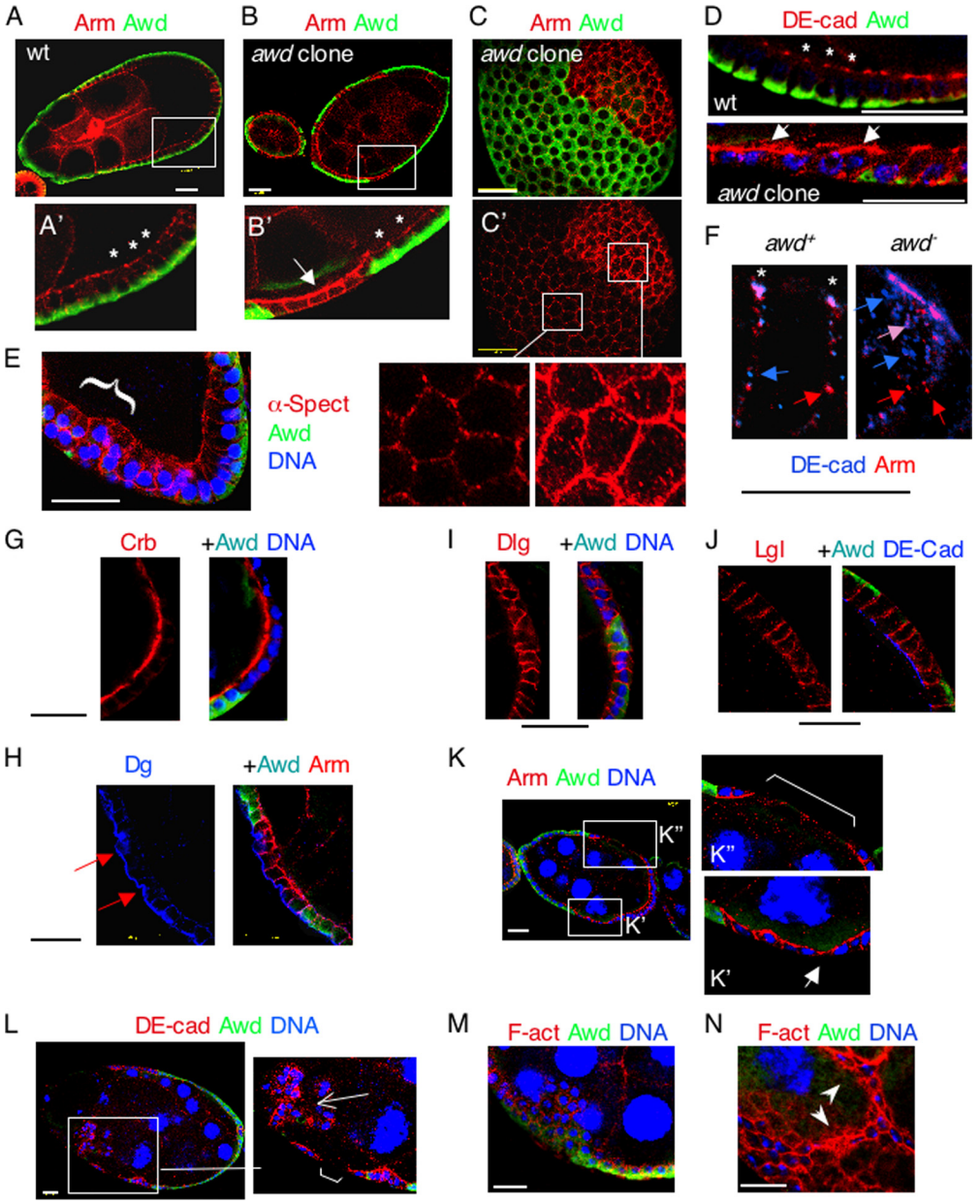

FIG. 3. *awd* mutant clones show a depolarized accumulation of adherens junction components and epithelial abnormalities. (A) Stage 9 wild-type (wt) egg chamber doubly stained for Awd (green) and Armadillo (Arm; red). (A′) The apicolateral membrane localization of Arm is highlighted (*). (B) *awd* mutant clones (arrow in B′) in a stage 8 egg, revealed by a lack of Awd staining (green). These mutant cells show an overaccumulation of Arm (red; arrow), while neighboring awd^+ cells show a typical apicolateral localization (*). (C) Surface optical cross-section of a stage 8 egg, showing double staining for Awd (green) and Arm (red). (C′) Staining of Arm alone. Arm overaccumulates on the *awd* mutant cell cortex. Close-up views show normal (left) and mutant (right) cells. Mutant cells contain an abundance of peripheral Arm and Arm-containing intracellular vesicles. (D) Enlarged views of a wild-type stage 8 egg chamber (top) with DE-cadherin (DE-cad) (red) at the apicolateral cell junctions (*). In the mutant clone (bottom), DE-cadherin spreads to the apical and lateral sides (arrows). Awd, green; To-Pro, blue. (E) Stage 10 egg chamber showing overaccumulation of α-spectrin (α-Spect) and a mild piling-up phenotype (brace). (F) Close-up views of awd^+ and awd^- stage 9 follicle cells, labeled for DE-cadherin (blue) and Arm (red). In the awd^+ cell, besides colocalization at the apicolateral adherens junctions (*), separate DE-cadherin and Arm are observed on the lateral cortex (blue and red arrows, respectively). In the awd^- cell, DE-cadherin and Arm colocalize to the apical membrane. In addition, cytoplasmic vesicles containing DE-cadherin (blue arrows), Arm (red arrows), or both (pink arrow) are identified. (G) A stage 7 egg chamber containing *awd* clones is stained for Crb, Awd, and DNA. Crb shows mild upregulation. (H) A stage 8 egg chamber containing *awd* clones is stained for Dg (blue), Awd (green), and Arm (red). Dg staining reveals a disrupted basal membrane (arrows), but the basal localization is not altered. (I) Stage 8 egg chamber stained for Dlg (red), Awd (green), and DNA (blue). (J) Stage 8 egg chamber stained for Lgl (red), Awd (green), and DE-cadherin (blue). Both basolateral markers show little change. (K) Stage 8 egg chamber showing stretched follicle cells (arrow in K′) and break-up of the epithelial sheet (bracket in K″). (L) Degenerating stage 9 egg chamber showing break-up of the epithelial sheet (bracket in inset) and severe piling up of follicle cells (arrow in inset). DE-cadherin, red; Awd, green; To-Pro, blue. (M and N) Stage 9 egg chambers containing *awd* clones are stained for F-actin (F-act) (phalloidin, red), Awd (green), and DNA (blue). (M) Adenoma-like epithelial expansion is observed. (N) In the most severe phenotype, large regions of the epithelium become multicell layered and invade deep into the germ cell complex (arrowheads). Bar, 20 μm.

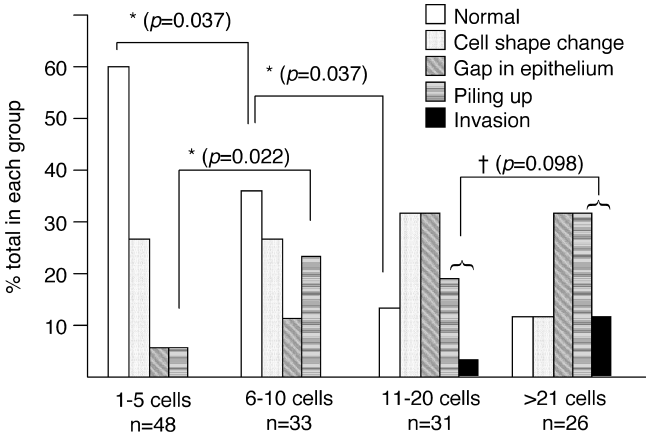

FIG. 4. Quantification of *awd* mutant phenotypes. The categories of phenotypes are described in the legend for Fig. 3. Phenotype distributions are tabulated separately according to the sizes of the clones. The cell number in each clone is counted from an optical cross-section through the center of the egg chamber. It is therefore not an actual total number of cells within a clone but a relative measurement of the clone size. *n* is the total number of clones examined within each group. Significant differences are indicated based on a two-sample *t* test for percentages (*, $P \leq 0.05$; †, $P \leq 0.1$).

with the size of the mutant clone. This is consistent with the notion that epithelial integrity is maintained by the junctions between the epithelial cell and its multiple neighbors.

Loss-of-function *awd* phenotypes in additional alleles. To confirm that the *awd* mutant clone phenotype is not due to unrelated genetic lesions present in the allele used, we examined another independent null (deletion) *awd* mutant allele, *KRS6* (46). The lethality of this allele is rescued by the *hsp-awd* transgene grown at 29°C. The surviving homozygous females were then shifted to 18°C for 3 days before egg chambers were dissected. Very few intact egg chambers were recovered. The few surviving egg chambers showed reduced and uneven Awd expression in the follicle cells (Fig. 5A and B). These egg chambers also display disrupted epithelial organization (Fig. 5A) and discontinuity of the epithelium (Fig. 5B). We should note that since Awd is needed for neuromuscular synaptic communication (23), residual Awd is required for keeping the adult females alive for ovary extraction; therefore, some Awd expression in ovaries is expected. But compared to the wild-type expression levels, the majority of mutant follicle cells indeed showed reduced expression (Fig. 5A and B, insets). Interestingly, we also observed increased staining for Awd in the germ cells (Fig. 5A and B), which are normally devoid of Awd expression in wild-type egg chambers. The ectopic expression is likely from the *hsp-awd* transgene expressed throughout ovary development, since awd^{KRS6} is a protein-null allele. Accumulation of exogenous Awd indicates that the germ cells cannot efficiently turn over ectopically expressed Awd. Also, as shown in Fig. 5B, there is one follicle cell that retained overexpressed Awd, while most of the other follicle cells surrounding the stretched epithelial locus showed reduced Awd expression.

To further confirm the *awd* loss-of-function phenotypes, we constructed a transgenic vector expressing an *awd*-specific RNA duplex (snap-back construct, awd^{sb}). A tail-to-tail duplex construct containing the first 150 nucleotides of the *awd* open reading frame was cloned into the expression vector under the heat shock (*hsp70*) promoter or *UAS* enhancer control. A sequence homology search confirmed that there is no nucleotide identity larger than 10 consecutive residues within this segment compared with the entire known *Drosophila* transcriptome. When the *awd* RNA duplex was induced by heat shock, clusters of *awd* knockdown cells could be identified (Fig. 5C). These cells showed an expected upregulation of Arm/β-catenin (Fig. 5C), DE-cadherin (data not shown), and α-spectrin (data not shown) and epithelial defects, such as multilayering of the epithelium. The awd^{sb}-induced knockdown effect was further confirmed using the *GAL4*/*UAS* binary system. When a *GAL4* line specifically expressed in the anterior of the columnar epithelium ($GAL4^{55B}$) (Fig. 5D) was used (30), clusters of *awd* knockdown cells could be detected (Fig. 5E to G). These *awd* knockdown cells exhibited overaccumulation of DE-cadherin (Fig. 5E), α-spectrin (Fig. 5F), and Arm (Fig. 5G) and a disorganized epithelial morphology. These analyses demonstrate that the epithelial phenotypes described are the specific result of *awd* loss of function.

Overexpression of Awd protein results in loss of epithelial characteristics. We next examined whether overexpression of Awd in follicle cells can result in reciprocal phenotypes. Two strategies were employed. First, the wild-type *awd* transgene was overexpressed from the *hsp70* promoter. The adult flies carrying the *hsp-awd* trangene were heat shocked at 37°C for 30 min twice a day for 3 days. This regimen generated Awd overexpression throughout the follicle cell body. These cells exhibit a profound cell shape change that is not seen in *awd* loss-of-function clones (Fig. 6A, compare to Fig. 3 and 5). The cells are swollen, rounded, or spindle shaped and become detached from their neighbors. They also cause disruption of neighboring cells. This morphological change is correlated with reduced membrane accumulation of Arm, as opposed to the increased accumulation of Arm observed for *awd* mutant clones.

In order to discern a subtler phenotype, the wild-type *awd* transgene was expressed from the $GAL4^{55B}$/*UAS* system (Fig. 6B). In this case, coexpressed LacZ was used to identify the overexpressing cells and show the overall cell shape (since Arm is expected to be diminished and Awd itself may not be overexpressed throughout the cell body). Identifiable LacZ-expressing cells exhibit abnormal cell shapes, with swelling and cellular projections. Therefore, downregulation or overexpression of Awd can cause different manifestations of epithelial defects. While the presence of Awd is required for the proper localization of adherens junction components, its overexpression also causes disruption of the same components. However, the phenotypic outcomes of loss of function and gain of function are quite different. *awd* loss of function produced a disorganized epithelium and piling up, but the epithelial cells remain adhered to the epithelium. Gain of function, on the other hand, generated detached epithelial cells that adopted mesenchymal-cell shapes. The latter is consistent with the loss of adherens junction components. However, neither loss of function nor gain of function of *awd* could generate epithelial-to-mesenchymal cell transition (EMT) or metastasis phenotypes; that is, no breakaway follicle cells were observed. It is also noteworthy

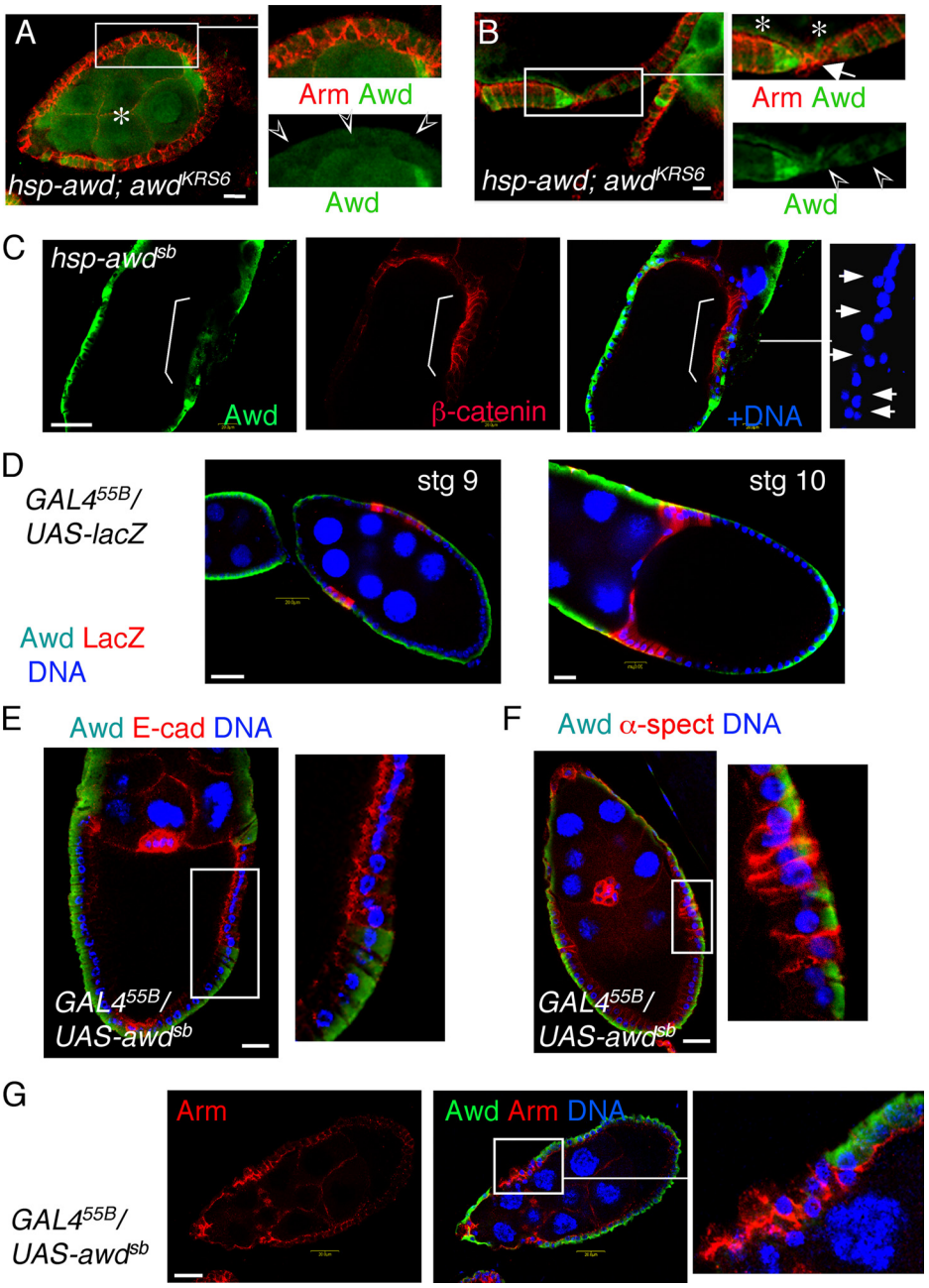

FIG. 5. Verification of *awd* loss-of-function mutant phenotypes. (A and B) awd^{KRS6} heterozygous flies carrying the *hsp-awd* rescue transgene were incubated at 29°C. Homozygous awd^{KRS6} female progenies were isolated and then conditioned at 18°C before dissection. Egg chambers show reduced Awd expression in the follicle cells (empty arrowheads) and a disrupted epithelium. Asterisks mark the ectopic expression of Awd in the germ cells. The arrow in panel B points to the stretched epithelium. One follicle cell shows ectopic expression of residual Awd among neighboring cells that show reduced Awd expression. (C to G) Female flies carrying $hsp\text{-}awd^{sb}$ (*awd* knockdown) (C), $GAL4^{55B}/UAS\text{-}lacZ$ (D), or $GAL4^{55B}/UAS\text{-}awd^{sb}$ (E to G) were dissected. The egg chambers were stained with the indicated antibodies and To-Pro. (C) In the stage 10 egg shown, the group of *awd* knockdown cells (bracket) can be identified clearly. These cells accumulate Arm (β-catenin; red) and show epithelial piling up (arrows in inset). (D) LacZ reporter expression pattern driven by $GAL4^{55B}$. Stage (stg) 9 and stage 10 eggs are stained for LacZ (red), Awd (green), and DNA (To-Pro, blue). LacZ is expressed in an anterior band of follicle cells. Note that in these cells the endogenous Awd expression is not affected and the follicle cells are normal. In $GAL4^{55B}/UAS\text{-}awd^{sb}$ egg chambers, overexpression of DE-cadherin (E-cad) (E), α-spectrin (α-spect) (F), and Arm (G) is observed. These *awd* knockdown cells also exhibit flattening (E), disorganized cell-cell contacts (F), and piling up (G). Bar, 20 μm.

that overexpression of a kinase-dead *awd* mutant (histidine 119 to alanine), which could not rescue the *awd* lethality (51), did not cause gain-of-function phenotypes (Fig. 7A and B), indicating that the phosphate transfer activity of Awd is critical for epithelial function.

We also examined the *Killer-of-prune* (*K-pn*) allele of *awd*, which carries a proline 97-to-serine mutation (P96S in the human protein). *K-pn* is a homozygous nonlethal, neomorphic allele that confers dominant lethality to the otherwise-nonlethal eye color mutant *prune* (6, 45). The cellular basis for this

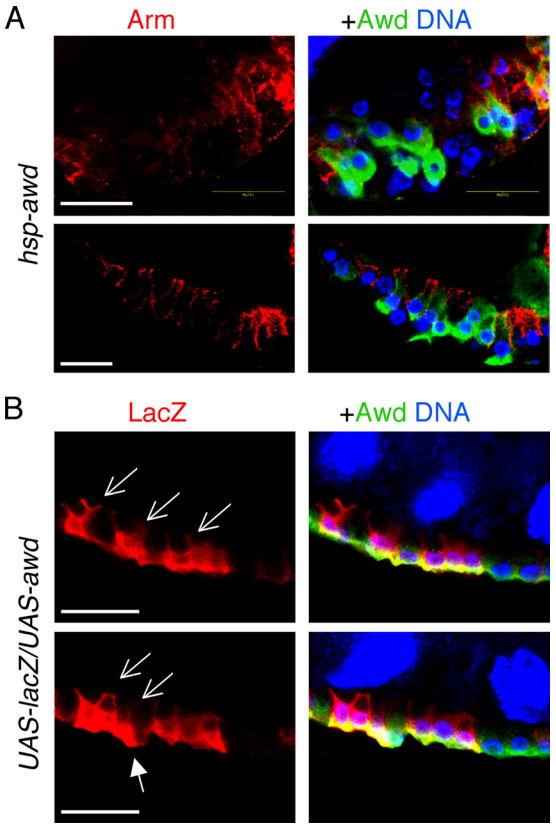

FIG. 6. Gain-of-function *awd* phenotypes. Female flies carrying *hsp-awd* (A) or $GAL4^{55B}$/*UAS-lacZ*/*UAS-awd* (B) were dissected. The egg chambers were stained with the indicated antibodies and To-Pro. (A) Portions of stage 9 egg chambers. *awd*-overexpressing cells are identified as those showing strong Awd staining (green) throughout the cytoplasm. Heat shock-induced Awd overexpression resulted in a dramatic cell shape change into rounded or spindle cells and severe disruption of the epithelium. (B) Portions of stage 9 egg chambers. *awd*-overexpressing cells are identified by the coexpression of LacZ. These cells show abnormal cellular projections (thin arrows) and a swollen shape (filled arrow). Bar, 20 μm.

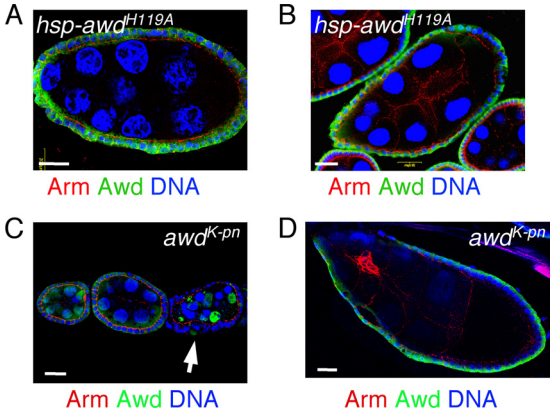

FIG. 7. Phosphate transfer activity is necessary for Awd function. (A and B) Females carrying the *hsp-awd*^{H119A} mutant transgene were heat treated as described in Results for Fig. 6A and dissected. The mutant Awd (green) is overexpressed throughout the cell bodies, but no epithelial phenotypes are observed. (C and D) Homozygous awd^{K-pn} females were dissected for ovaries. Some degenerate egg chambers were found at early stages (arrow), but no overt epithelial phenotypes in other egg chambers are observed. Bar, 20 μm.

phenotype is unknown. However, it has been shown that both human and *Drosophila* K-pn mutant proteins retain nucleoside diphosphate kinase activity but that the human K-pn protein is defective in protein kinase activity (15, 25). Structural studies indicate that the mutant protein is more flexible and exhibits reduced stability in response to heat treatment or denaturing agents (25, 47). Interestingly, awd^{K-pn} ovaries showed occasional degenerating egg chambers at early stages (5% of ovarioles, $n = 46$) but no significant epithelial defects (Fig. 7C and D). If the previous analysis of the enzymatic function of the human K-pn protein also holds true for the *Drosophila* counterpart, our observation suggests that the epithelial function of Awd is dependent on the nucleoside diphosphate kinase activity and not on the protein kinase activity. However, whether Awd possesses the protein kinase function needs to be tested vigorously in future studies.

***awd* functionally interacts with *Rab5*.** Figure 3C shows that *awd* mutant cells accumulate Arm-containing vesicles. Since endocytosis of the adherens junction components is critical for the homeostasis of the junctional complex (52), particularly during epithelial reorganization, we suspect that the accumulation of the DE-cadherin–Armadillo complex may be the result of defects in the endocytic pathway. Surface accumulation of Arm may be the result of defective early-endosome formation or enhanced recycling. Accumulation of Arm-containing cytoplasmic vesicles, as shown in Fig. 3C and F, indicates that the first step in the endocytic pathway catalyzed by dynamin—cleavage of endocytic-vesicle invagination—is functional. Overabundance of endocytic vesicles in the *awd* mutant cells is also inconsistent with an enhanced recycling pathway. Indeed, ectopic expression of CA or DN Rab11 (a central component in the recycling endosomes) did not induce any epithelial phenotypes (see Fig. S2B in the supplemental material). A previous report has shown that Nm23-H1 is recruited by Arf6 GTPase to the adherens junction and promotes internalization of E-cadherin in Madin-Darby canine kidney (MDCK) cells (40). We therefore also tested whether Arf6 plays a role in follicle cell morphogenesis. As shown in Fig. S2C in the supplemental material, neither CA nor DN mutants of Arf6 could induce epithelial phenotypes when ectopically expressed in the follicle cell. These negative results prompted us to examine the role of Rab5, a key component in promoting endocytic-vesicle fusion with early endosomes. We tabulated the phenotypes resulting from overexpression of wild-type *Rab5*, DN *Rab5* (the S43N mutant), or CA *Rab5* (the Q88L mutant) and compared them with the phenotypes generated by overexpressing the awd^{sb} (knockdown) construct. It has been shown that wild-type and CA YFP-Rab5 proteins are localized to the early endosomes, while the DN fusion protein is mislocalized (53). *UAS*-driven transgenes were activated by the anterior-follicle-cell-specific GAL^{55B} line, as described for Fig. 5D and Fig. S2A in the supplemental material. awd^{sb} was then combined with each of the *Rab5* variants to elucidate the possible genetic interactions. A neutral *UAS-lacZ* transgene was used as a negative control and was coexpressed with the awd^{sb} or *Rab5* transgene to normalize the available dosage of GAL4. The distribution of phenotypes is summarized in Table 1.

$Rab5^{S43N}$ (DN) produced modest *awd* loss-of-function phe-

TABLE 1. *awd* and *Rab5* genetic interactions

Transgene combination	n^a	% with phenotype					
		Normal	Cell shape change		Epithelial gap	Piling up/ loose cells	Invasion
			Flattening	Spindle/ swelling			
lacZ	52	96	4				
awd^{sb} plus *lacZ*	44	25	30		11	27	7
$Rab5^{wt}$ plus *lacZ*	19	84		11		5	
$Rab5^{Q88L}$ plus *lacZ*	21	86		14			
$Rab5^{S43N}$ plus *lacZ*	35	77	14			9	
$Rab5^{wt}$ plus awd^{sb}	54	61	4	9	4	22	
$Rab5^{Q88L}$ plus awd^{sb}	37	73	3	19	5		
$Rab5^{S43N}$ plus awd^{sb}	37	24	35		19	19	3

[a] *n*, number of clusters of epithelial cells in a cross-section expressing the indicated transgene(s).

notypes (14% cell flattening and 9% piling up), while $Rab5^{wt}$ (wild type) and $Rab5^{Q88L}$ (CA) generated appreciable phenotypes of cell swelling (11% and 14%, respectively) that are reminiscent of the *awd*-overexpressing phenotype. awd^{sb} by itself generated significant loss-of-function phenotypes (30% flattened cell shape, 11% epithelial gap, and 34% combined piling up and invasion). When these *Rab5* transgenes were combined with awd^{sb}, it was observed that awd^{sb} (loss-of-function) phenotypes were rescued by $Rab5^{wt}$ and $Rab5^{Q88L}$. The value of 25% normal egg chambers produced by awd^{sb} was increased to 61% and 73% in the presence of $Rab5^{wt}$ and $Rab5^{Q88L}$, respectively ($P = 0.0006$ and $P < 0.0001$). The combined severe phenotypes (piling up and invasion) were reduced from 34% to 22% and 0% for $Rab5^{wt}$ and $Rab5^{Q88L}$, respectively ($P = 0.188$ and $P = 0.002$). Therefore, wild-type Rab5 could rescue the mild phenotypes, such as cell shape change and epithelial gaps, but was less effective than CA Rab5 in rescuing severe phenotypes, such as piling up and invasion (22% compared with 0%, respectively; $P = 0.029$). We conclude that Awd and Rab5 are agonists in promoting endocytosis of the adherens junction components. Interestingly, DN *Rab5* ($Rab5^{S43N}$) did not exacerbate the *awd* knockdown phenotype. The combined $Rab5^{S43N}$ and awd^{sb} phenotype remained at the same level of severity as that for awd^{sb} alone. This suggests that Awd is critical for Rab5 function. Without Awd activity, DN Rab5 cannot further inhibit the endocytic function. The modest phenotypes generated by overexpressing wild-type and CA Rab5 indicate the presence of auxiliary endocytic components that can modulate the Rab5 function. For example, the availability of other endosomal components, such as the Sec1/Munc18 family protein Vps45 and the syntaxin Avalanche, can limit the function of Rab5 (34). The severity of the Awd overexpression phenotypes compared to the mildness of the Rab5 and CA Rab5 overexpression phenotypes also indicates that Awd may regulate multiple endocytic-pathway components.

***awd* regulates the expression level of Rab5.** During examination of the *YFP-Rab5* transgene- and awd^{sb}-induced phenotypes, we noted interesting expression patterns of the YFP-Rab5 fusion proteins (Fig. 8A). First, the wild type is expressed throughout the cytoplasm, while CA Rab5 is in large aggregates, presumably the enlarged endosomes due to overactive endosome fusion. In contrast, DN Rab5 is expressed at a lower level in small, dispersed puncta. Interestingly, when coexpressed with awd^{sb}, wild-type and DN Rab5 were greatly reduced, while CA Rab5 remained in large aggregates. These results indicate that *awd* may be needed to stabilize the inactive, cytosolic pool of Rab5. To further test this notion, we examined the endogenous Rab5 expression pattern in *awd* mutant clones. Incredibly, endogenous Rab5 is downregulated in *awd* mutant cells (Fig. 8B).

DISCUSSION

We report here, for the first time, a novel function for the *Nm23* gene family in epithelial morphogenesis in vivo. Our data suggest that Awd promotes internalization of the adherens junction components, such as DE-cadherin and β-catenin (Armadillo), and that this activity is mediated via the function of Rab5.

Rab5 has been shown to promote internalization of DE-cadherin and the apical complex protein Crb in the imaginal discs (26). Interestingly, we observed only a mild increase of apical Crb levels in *awd* mutant cells, suggesting that Crb is less reliant on Rab5-Awd-mediated endocytosis in the follicle cells. Nm23-H1 has been shown to promote E-cadherin endocytosis in canine kidney tubule MDCK cells (40). This function appears to be consistent with the *awd* mutant phenotypes reported here. These authors identified Arf6 as a mediator of Nm23 function. However, we determined that Arf6 played no roles in our in vivo model. Whether this discrepancy is due to different cell contexts or evolutionary divergence remains to be determined.

Our results suggest that the expression of the Awd protein needs to be within a tightly controlled range both quantitatively and spatially to maintain epithelial homeostasis. We propose that the role of Awd in the follicle cells is to downregulate the mislocalized E-cadherin–β-catenin complex from the membrane. Mislocalized adherens junction components are present before the epithelial junctions are firmly established (before stage 6) and during epithelial-sheet movement at stage 9, which requires active turnover of the adherens junctions. In early egg chambers, before the epithelial polarity is completely established, Awd is needed in the apical and lateral domains to remove the unengaged E-cadherin and Arm. After stage 6, when membrane domains are established and the apical membrane is sealed from the lateral domain by the Crb-containing apical complex, Awd relocalizes to the basolateral region and continues to retrieve laterally localized, uncomplexed adherens

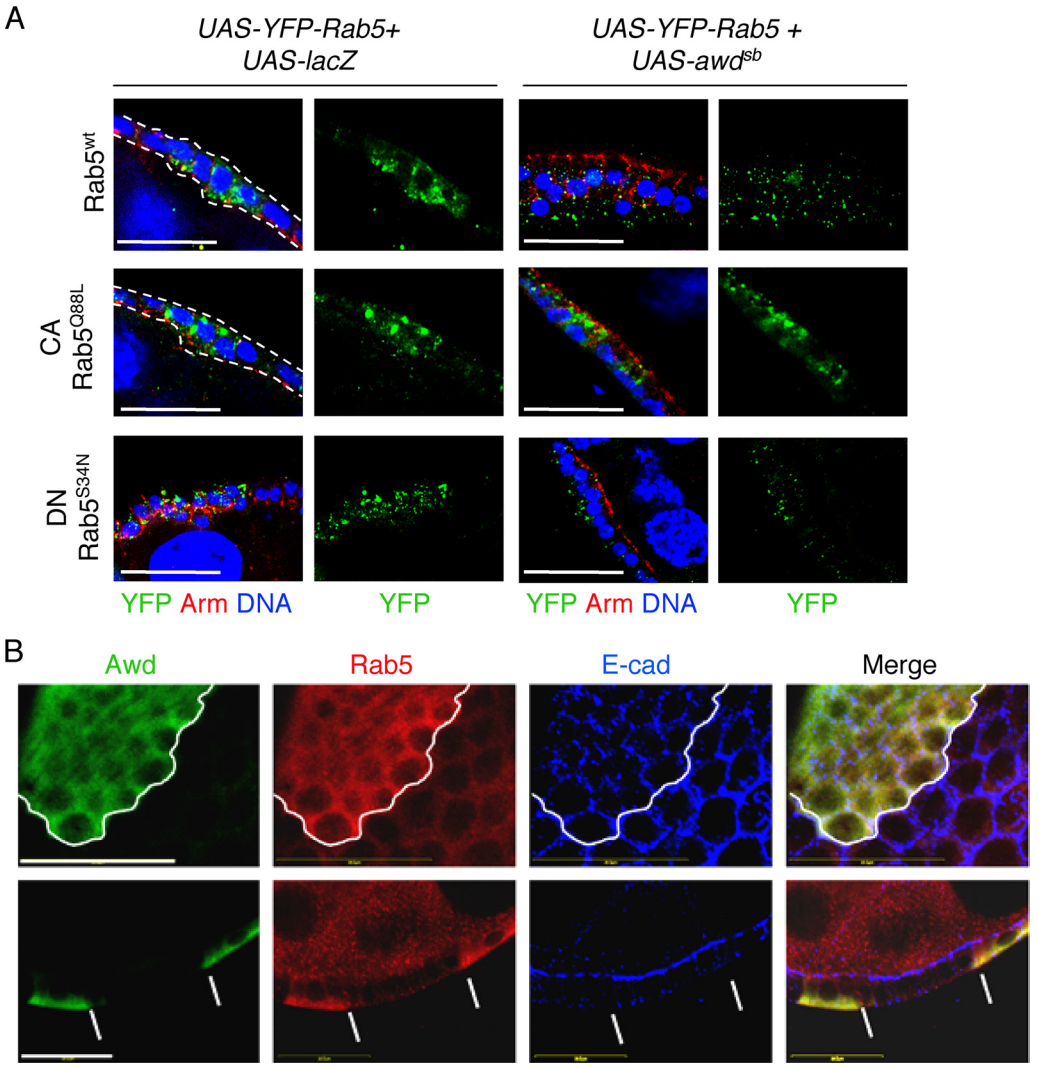

FIG. 8. Rab5 is downregulated in *awd* mutant cells. (A) Female flies carrying GAL^{55B} and the indicated *UAS* transgenes were dissected and processed for staining with the indicated antibodies and To-Pro. In the examples shown, wild-type Rab5 and CA Rab5 generated mild cell swelling (dashed lines), while DN Rab5 generated piling up. *awd* knockdown resulted in reduced levels of wild-type and DN Rab5 but not of CA Rab5. YFP, green; Arm, red; DNA, blue. (B) *awd* mutant clones were generated as described in Materials and Methods. Ovaries were dissected and stained for Awd (green), *Drosophila* Rab5 (red), and DE-cadherin (E-cad) (blue). Top panels show the surface view of a stage 8 egg chamber. Bottom panels show a cross-section of another stage 8 egg chamber. Lines mark the boundaries between Awd-expressing and null cells. In *awd* null cells, DE-cadherin is upregulated, as expected, and Rab5 is significantly downregulated. Bar, 20 μm.

junction components. Our results showed that ectopic overexpression of Awd, which resulted in the spread of Awd throughout the cytoplasm at later stages, could reduce adherens junctions and generated a spindle cell shape. This indicates that overexpression of Awd can also promote turnover of the engaged adherens junction components. The overexpression-induced phenotype can therefore be considered an oncogenic function of this metastasis suppressor. This model can explain the conflicting results in correlating *Nm23* expression levels with cancer prognosis. It should be emphasized that loss of function and overexpression of *awd* generated different manifestations of epithelial defects. Loss of function of *awd* resulted in the overaccumulation of adherens junction components and adenoma-like piling up, but the mutant cells remained adhered to the neighbors. Overexpression, on the other hand, resulted in profound cell shape changes into shapes that resemble those of mesenchymal cells, but these cells did not escape from the epithelium. In fact, we never observed breakaway epithelial cells that mimic metastasis under either condition. Therefore, the EMT is not generated in either *awd* loss-of-function or *awd* gain-of-function mutants. The most prevailing EMT molecular marker is E-cadherin, which is shown to accumulate in *awd* mutant cells and to come off the membrane in *awd*-overexpressing cells. This confirms the notion that the loss of E-cadherin is necessary but not sufficient for the EMT. In support of this, other EMT markers examined here, such as Dlg and Lgl, did not show alterations. We believe that to generate the EMT phenotype the epithelial cells need to be induced to migrate or possess intrinsic migratory potential. Such conditions can be observed with border cell and tracheal-cell migra-

tion, as we have described previously (8, 36). With border cells, *awd* downregulation is needed for the invasive movement, but the migration requires delamination from the epithelium a priori, which is not regulated by *awd*. In *Drosophila* tracheal cells, which normally migrate in response to the chemotactic FGF signaling, *awd* loss-of-function mutations resulted in EMT-like, rounded cells delaminated from the tubule epithelium. Thus, *awd* mutation can indeed generate the EMT phenotype, albeit only in cells with intrinsic motility.

One confounding factor that hinders the elucidation of the Nm23 pathophysiological function is the multitude of enzymatic activities identified: (i) nucleoside diphosphate kinase activity, which transfers the terminal phosphate group from ATP to a nucleoside diphosphate (such as GDP) through the formation of an intermediate histidine-phosphate linkage at histidine 118 (residue 119 in *Drosophila*) (38); (ii) DNA binding and DNA nuclease activities, which are involved in transcriptional regulation (27, 41); (iii) DNase activity, which is activated by granzyme A in caspase-independent apoptosis (14); and (iv) histidine-dependent protein kinase activity (13, 21, 49). The protein kinase enzymatic activity is similar to that of nucleoside diphosphate kinase but toward protein substrates (4). Some tantalizing kinase targets, such as aldolase C and kinase suppressor of Ras (Ksr), have been identified, but the in vivo relevance of these targets requires further investigation (44). It has been suggested that it is the protein kinase activity that is important for the antimetastasis function of Nm23 (15, 28). However, these non-nucleoside diphosphate kinase activities have not been verified in vivo. Furthermore, we have never observed nucleus-localized Awd in wild-type follicle cells. This makes the transcription regulator or DNase activities for Awd less likely, at least in the follicle cell system.

Since Nm23 is a potential GTP supplier, it has been proposed as an agonist for various cellular GTPases. Among the best-studied interactors of Nm23 in mammalian cells, many are indeed related directly or indirectly to the GTPases, such as Arf6 (40), TIAM1 (GEF [guanine nucleotide exchange factor] for Rac) (37), Lbc (GEF for Rho) (22), and Rad (48). These interacting proteins can potentially provide a mechanism for the function of Nm23 in regulating cell motility and endocytosis. However, while Arf6 is an Nm23 functional partner, other GTPase functions mentioned above are inhibited by Nm23, thus excluding the GTPase agonist function. These various partners may function in different cell types or in different cellular processes. The *Drosophila* developmental systems relevant to Nm23 functions—neurotransmission, tracheal branching, border cell migration, and follicular epithelial morphogenesis—should provide an excellent model for testing these functional relationships in future studies.

Previously, the endocytic function of *awd* has been shown to interact with *dynamin/shibire* (8, 23, 36). This indicates that Awd functions in the dynamin-dependent endocytic pathway but does not necessitate a direct regulatory role of Awd on dynamin activity. Indeed, with the follicle cell system reported here, we observed defective endocytosis correlating with an abundance of endocytic vesicles in the cytoplasm of *awd* mutant cells. This suggests that Awd does not directly regulate dynamin function, the loss of which should result in a lack of endocytic-vesicle formation. Also, it is unlikely that Awd physically interacts with either DE-cadherin or Arm because Awd does not colocalize with these proteins in the vesicles. Instead, we demonstrated that the level of wild-type Rab5 protein, which promotes delivery of endocytic vesicles to the early endosome, is diminished in *awd* mutant cells. Interestingly, while wild-type and DN Rab5 proteins are unstable, CA Rab5 appears to be stable in *awd* knockdown cells. These results suggest that Awd may be a chaperone protein that protects inactive Rab5. This function may be mediated by a perceived GTP supplier role of the Nm23 proteins (via its nucleoside diphosphate kinase activity), although it has not been documented that the availability of GTP can influence the levels of Ras-like proteins. We determined that the substitution mutation that replaced the critical histidine residue could not induce follicle cell phenotypes when overexpressed. Since the histidine residue is important for both nucleoside diphosphate kinase and putative protein kinase activities, it is currently unresolved which enzymatic activity is responsible for the reported epithelial function. The *Drosophila* systems should provide a platform for future mutational studies that will elucidate the critical enzymatic function of the Nm23 family of proteins.

ACKNOWLEDGMENTS

We thank Crislyn D'Souza-Schorey for providing the Arf6 transgenes, Wu-Min Deng for providing the anti-Dg antibody, and Daniela Grifoni for providing the anti-Lgl antibody.

This work was supported by a grant from the National Institutes of Health to T.H. (RO1GM57843).

REFERENCES

1. **An, H. J., D. S. Kim, Y. K. Park, S. K. Kim, Y. P. Choi, S. Kang, B. Ding, and N. H. Cho.** 2006. Comparative proteomics of ovarian epithelial tumors. J. Proteome Res. **5:**1082–1090.
2. **Anwar, S., I. M. Frayling, N. A. Scott, and G. L. Carlson.** 2004. Systematic review of genetic influences on the prognosis of colorectal cancer. Br. J. Surg. **91:**1275–1291.
3. **Arnaud-Dabernat, S., P. M. Bourbon, A. Dierich, M. Le Meur, and J. Y. Daniel.** 2003. Knockout mice as model systems for studying nm23/NDP kinase gene functions. Application to the nm23-M1 gene. J. Bioenerg. Biomembr. **35:**19–30.
4. **Besant, P. G., E. Tan, and P. V. Attwood.** 2003. Mammalian protein histidine kinases. Int. J. Biochem. Cell Biol. **35:**297–309.
5. **Biggs, J., E. Hersperger, P. S. Steeg, L. A. Liotta, and A. Shearn.** 1990. A Drosophila gene that is homologous to a mammalian gene associated with tumor metastasis codes for a nucleoside diphosphate kinase. Cell **63:**933–940.
6. **Biggs, J., N. Tripoulas, E. Hersperger, C. Dearolf, and A. Shearn.** 1988. Analysis of the lethal interaction between the prune and Killer of prune mutations of Drosophila. Genes Dev. **2:**1333–1343.
7. **Boissan, M., D. Wendum, S. Arnaud-Dabernat, A. Munier, M. Debray, I. Lascu, J. Y. Daniel, and M. L. Lacombe.** 2005. Increased lung metastasis in transgenic NM23-Null/SV40 mice with hepatocellular carcinoma. J. Natl. Cancer Inst. **97:**836–845.
8. **Dammai, V., B. Adryan, K. R. Lavenburg, and T. Hsu.** 2003. Drosophila awd, the homolog of human nm23, regulates FGF receptor levels and functions synergistically with shi/dynamin during tracheal development. Genes Dev. **17:**2812–2824.
9. **Dearolf, C. R., E. Hersperger, and A. Shearn.** 1988. Developmental consequences of awdb3, a cell-autonomous lethal mutation of Drosophila induced by hybrid dysgenesis. Dev. Biol. **129:**159–168.
10. **Dearolf, C. R., N. Tripoulas, J. Biggs, and A. Shearn.** 1988. Molecular consequences of awdb3, a cell-autonomous lethal mutation of Drosophila induced by hybrid dysgenesis. Dev. Biol. **129:**169–178.
11. **Deng, W. M., M. Schneider, R. Frock, C. Castillejo-Lopez, E. A. Gaman, S. Baumgartner, and H. Ruohola-Baker.** 2003. Dystroglycan is required for polarizing the epithelial cells and the oocyte in Drosophila. Development **130:**173–184.
12. **Dobens, L. L., and L. A. Raftery.** 2000. Integration of epithelial patterning and morphogenesis in Drosophila ovarian follicle cells. Dev. Dyn. **218:**80–93.
13. **Engel, M., M. Veron, B. Theisinger, M. L. Lacombe, T. Seib, S. Dooley, and C. Welter.** 1995. A novel serine/threonine-specific protein phosphotransferase activity of Nm23/nucleoside-diphosphate kinase. Eur. J. Biochem. **234:**200–207.

14. **Fan, Z., P. J. Beresford, D. Y. Oh, D. Zhang, and J. Lieberman.** 2003. Tumor suppressor NM23-H1 is a granzyme A-activated DNase during CTL-mediated apoptosis, and the nucleosome assembly protein SET is its inhibitor. Cell **112:**659–672.
15. **Freije, J. M., P. Blay, N. J. MacDonald, R. E. Manrow, and P. S. Steeg.** 1997. Site-directed mutation of Nm23-H1. Mutations lacking motility suppressive capacity upon transfection are deficient in histidine-dependent protein phosphotransferase pathways in vitro. J. Biol. Chem. **272:**5525–5532.
16. **Galani, E., J. Sgouros, C. Petropoulou, J. Janinis, G. Aravantinos, D. Dionysiou-Asteriou, D. Skarlos, and E. Gonos.** 2002. Correlation of MDR-1, nm23-H1 and H Sema E gene expression with histopathological findings and clinical outcome in ovarian and breast cancer patients. Anticancer Res. **22:**2275–2280.
17. **Galbiati, F., D. Volonte, A. M. Brown, D. E. Weinstein, A. Ben-Ze'ev, R. G. Pestell, and M. P. Lisanti.** 2000. Caveolin-1 expression inhibits Wnt/beta-catenin/Lef-1 signaling by recruiting beta-catenin to caveolae membrane domains. J. Biol. Chem. **275:**23368–23377.
18. **Grifoni, D., F. Garoia, C. C. Schimanski, G. Schmitz, E. Laurenti, P. R. Galle, A. Pession, S. Cavicchi, and D. Strand.** 2004. The human protein Hugl-1 substitutes for Drosophila lethal giant larvae tumour suppressor function in vivo. Oncogene **23:**8688–8694.
19. **Harlozinska, A., J. K. Bar, and J. Gerber.** 1996. nm23 expression in tissue sections and tumor effusion cells of ovarian neoplasms. Int. J. Cancer **69:** 415–419.
20. **Heimann, R., and S. Hellman.** 2000. Individual characterisation of the metastatic capacity of human breast carcinoma. Eur. J. Cancer **36:**1631–1639.
21. **Inoue, H., M. Takahashi, A. Oomori, M. Sekiguchi, and T. Yoshioka.** 1996. A novel function for nucleoside diphosphate kinase in Drosophila. Biochem. Biophys. Res. Commun. **218:**887–892.
22. **Iwashita, S., M. Fujii, H. Mukai, Y. Ono, and M. Miyamoto.** 2004. Lbc proto-oncogene product binds to and could be negatively regulated by metastasis suppressor nm23-H2. Biochem. Biophys. Res. Commun. **320:**1063–1068.
23. **Krishnan, K. S., R. Rikhy, S. Rao, M. Shivalkar, M. Mosko, R. Narayanan, P. Etter, P. S. Estes, and M. Ramaswami.** 2001. Nucleoside diphosphate kinase, a source of GTP, is required for dynamin-dependent synaptic vesicle recycling. Neuron **30:**197–210.
24. **Lacombe, M. L., L. Milon, A. Munier, J. G. Mehus, and D. O. Lambeth.** 2000. The human Nm23/nucleoside diphosphate kinases. J. Bioenerg. Biomembr. **32:**247–258.
25. **Lascu, I., A. Chaffotte, B. Limbourg-Bouchon, and M. Veron.** 1992. A Pro/Ser substitution in nucleoside diphosphate kinase of Drosophila melanogaster (mutation killer of prune) affects stability but not catalytic efficiency of the enzyme. J. Biol. Chem. **267:**12775–12781.
26. **Lu, H., and D. Bilder.** 2005. Endocytic control of epithelial polarity and proliferation in Drosophila. Nat. Cell Biol. **7:**1232–1239.
27. **Ma, D., Z. Xing, B. Liu, N. G. Pedigo, S. G. Zimmer, Z. Bai, E. H. Postel, and D. M. Kaetzel.** 2002. NM23-H1 and NM23-H2 repress transcriptional activities of nuclease-hypersensitive elements in the platelet-derived growth factor-A promoter. J. Biol. Chem. **277:**1560–1567.
28. **MacDonald, N. J., J. M. Freije, M. L. Stracke, R. E. Manrow, and P. S. Steeg.** 1996. Site-directed mutagenesis of nm23-H1. Mutation of proline 96 or serine 120 abrogates its motility inhibitory activity upon transfection into human breast carcinoma cells. J. Biol. Chem. **271:**25107–25116.
29. **Mandai, M., I. Konishi, M. Koshiyama, T. Mori, S. Arao, H. Tashiro, H. Okamura, H. Nomura, H. Hiai, and M. Fukumoto.** 1994. Expression of metastasis-related nm23-H1 and nm23-H2 genes in ovarian carcinomas: correlation with clinicopathology, EGFR, c-erbB-2, and c-erbB-3 genes, and sex steroid receptor expression. Cancer Res. **54:**1825–1830.
30. **Manseau, L., A. Baradaran, D. Brower, A. Budhu, F. Elefant, H. Phan, A. V. Philp, M. Yang, D. Glover, K. Kaiser, K. Palter, and S. Selleck.** 1997. GAL4 enhancer traps expressed in the embryo, larval brain, imaginal discs, and ovary of Drosophila. Dev. Dyn. **209:**310–322.
31. **Mantrova, E. Y., R. A. Schulz, and T. Hsu.** 1999. Oogenic function of the myogenic factor D-MEF2: negative regulation of the decapentaplegic receptor gene thick veins. Proc. Natl. Acad. Sci. USA **96:**11889–11894.
32. **Meng, W., Y. Mushika, T. Ichii, and M. Takeichi.** 2008. Anchorage of microtubule minus ends to adherens junctions regulates epithelial cell-cell contacts. Cell **135:**948–959.
33. **Mochizuki, T., A. Bilitou, C. T. Waters, K. Hussain, M. Zollo, and S. Ohnuma.** 2009. Xenopus NM23-X4 regulates retinal gliogenesis through interaction with p27Xic1. Neural Dev. **4:**1.
34. **Morrison, H. A., H. Dionne, T. E. Rusten, A. Brech, W. W. Fisher, B. D. Pfeiffer, S. E. Celniker, H. Stenmark, and D. Bilder.** 2008. Regulation of early endosomal entry by the Drosophila tumor suppressors Rabenosyn and Vps45. Mol. Biol. Cell **19:**4167–4176.
35. **Nallamothu, G., V. Dammai, and T. Hsu.** 2009. Developmental function of Nm23/awd-A mediator of endocytosis. Mol. Cell. Biochem. [Epub ahead of print.] doi:10.1007/s11010-009-0112-7.
36. **Nallamothu, G., J. A. Woolworth, V. Dammai, and T. Hsu.** 2008. Awd, the homolog of metastasis suppressor gene Nm23, regulates *Drosophila* epithelial cell invasion. Mol. Cell. Biol. **28:**1964–1973.
37. **Otsuki, Y., M. Tanaka, S. Yoshii, N. Kawazoe, K. Nakaya, and H. Sugimura.** 2001. Tumor metastasis suppressor nm23H1 regulates Rac1 GTPase by interaction with Tiam1. Proc. Natl. Acad. Sci. USA **98:**4385–4390.
38. **Ouatas, T., M. Salerno, D. Palmieri, and P. S. Steeg.** 2003. Basic and translational advances in cancer metastasis: Nm23. J. Bioenerg. Biomembr. **35:**73–79.
39. **Ouellet, V., C. Le Page, M. C. Guyot, C. Lussier, P. N. Tonin, D. M. Provencher, and A. M. Mes-Masson.** 2006. SET complex in serous epithelial ovarian cancer. Int. J. Cancer **119:**2119–2126.
40. **Palacios, F., J. K. Schweitzer, R. L. Boshans, and C. D'Souza-Schorey.** 2002. ARF6-GTP recruits Nm23-H1 to facilitate dynamin-mediated endocytosis during adherens junctions disassembly. Nat. Cell Biol. **4:**929–936.
41. **Postel, E. H., S. J. Berberich, J. W. Rooney, and D. M. Kaetzel.** 2000. Human NM23/nucleoside diphosphate kinase regulates gene expression through DNA binding to nuclease-hypersensitive transcriptional elements. J. Bioenerg. Biomembr. **32:**277–284.
42. **Sirotkovic-Skerlev, M., S. Krizanac, S. Kapitanovic, K. Husnjak, J. Unusic, and K. Pavelic.** 2005. Expression of c-myc, erbB-2, p53 and nm23-H1 gene product in benign and malignant breast lesions: coexpression and correlation with clinicopathologic parameters. Exp. Mol. Pathol. **79:**42–50.
43. **Steeg, P. S., G. Bevilacqua, L. Kopper, U. P. Thorgeirsson, J. E. Talmadge, L. A. Liotta, and M. E. Sobel.** 1988. Evidence for a novel gene associated with low tumor metastatic potential. J. Natl. Cancer Inst. **80:**200–204.
44. **Steeg, P. S., D. Palmieri, T. Ouatas, and M. Salerno.** 2003. Histidine kinases and histidine phosphorylated proteins in mammalian cell biology, signal transduction and cancer. Cancer Lett. **190:**1–12.
45. **Sturtevant, A. H.** 1956. A highly specific complementary lethal system in Drosophila melanogaster. Genetics **41:**118–123.
46. **Timmons, L., E. Hersperger, E. Woodhouse, J. Xu, L. Z. Liu, and A. Shearn.** 1993. The expression of the Drosophila awd gene during normal development and in neoplastic brain tumors caused by lgl mutations. Dev. Biol. **158:**364–379.
47. **Timmons, L., J. Xu, G. Hersperger, X. F. Deng, and A. Shearn.** 1995. Point mutations in awdKpn which revert the prune/Killer of prune lethal interaction affect conserved residues that are involved in nucleoside diphosphate kinase substrate binding and catalysis. J. Biol. Chem. **270:**23021–23030.
48. **Tseng, Y. H., D. Vicent, J. Zhu, Y. Niu, A. Adeyinka, J. S. Moyers, P. H. Watson, and C. R. Kahn.** 2001. Regulation of growth and tumorigenicity of breast cancer cells by the low molecular weight GTPase Rad and nm23. Cancer Res. **61:**2071–2079.
49. **Wagner, P. D., P. S. Steeg, and N. D. Vu.** 1997. Two-component kinase-like activity of nm23 correlates with its motility-suppressing activity. Proc. Natl. Acad. Sci. USA **94:**9000–9005.
50. **Wallet, V., R. Mutzel, H. Troll, O. Barzu, B. Wurster, M. Veron, and M. L. Lacombe.** 1990. Dictyostelium nucleoside diphosphate kinase highly homologous to Nm23 and Awd proteins involved in mammalian tumor metastasis and Drosophila development. J. Natl. Cancer Inst. **82:**1199–1202.
51. **Xu, J., L. Z. Liu, X. F. Deng, L. Timmons, E. Hersperger, P. S. Steeg, M. Veron, and A. Shearn.** 1996. The enzymatic activity of Drosophila AWD/NDP kinase is necessary but not sufficient for its biological function. Dev. Biol. **177:**544–557.
52. **Yap, A. S., M. S. Crampton, and J. Hardin.** 2007. Making and breaking contacts: the cellular biology of cadherin regulation. Curr. Opin. Cell Biol. **19:**508–514.
53. **Zhang, J., K. L. Schulze, P. R. Hiesinger, K. Suyama, S. Wang, M. Fish, M. Acar, R. A. Hoskins, H. J. Bellen, and M. P. Scott.** 2007. Thirty-one flavors of Drosophila rab proteins. Genetics **176:**1307–1322.